



# Kent Academic Repository

**Shastri, Anshuman, Ullah, Irfan and Sanz-Izquierdo, Benito (2021) *Alternating Current Sensing Slot Antenna*. IEEE Sensors Journal, 21 (7). pp. 9484-9491. ISSN 1530-437X.**

## Downloaded from

<https://kar.kent.ac.uk/87447/> The University of Kent's Academic Repository KAR

## The version of record is available from

<https://doi.org/10.1109/JSEN.2021.3055639>

## This document version

Author's Accepted Manuscript

## DOI for this version

## Licence for this version

UNSPECIFIED

## Additional information

## Versions of research works

### Versions of Record

If this version is the version of record, it is the same as the published version available on the publisher's web site. Cite as the published version.

### Author Accepted Manuscripts

If this document is identified as the Author Accepted Manuscript it is the version after peer review but before type setting, copy editing or publisher branding. Cite as Surname, Initial. (Year) 'Title of article'. To be published in *Title of Journal*, Volume and issue numbers [peer-reviewed accepted version]. Available at: DOI or URL (Accessed: date).

## Enquiries

If you have questions about this document contact [ResearchSupport@kent.ac.uk](mailto:ResearchSupport@kent.ac.uk). Please include the URL of the record in KAR. If you believe that your, or a third party's rights have been compromised through this document please see our [Take Down policy](https://www.kent.ac.uk/guides/kar-the-kent-academic-repository#policies) (available from <https://www.kent.ac.uk/guides/kar-the-kent-academic-repository#policies>).

# Alternating Current Sensing Slot Antenna

Anshuman Shastri, Irfan Ullah, and Benito Sanz-Izquierdo

**Abstract**— Dual operations of AC current sensing and Bluetooth transmission using a reconfigurable slot antenna are described here. The novel current sensing setup comprises of a tunable antenna connected to a current transformer and AC/DC converter to create a smart AC current sensing mechanism. The tunable antenna consists of a double-layer slot antenna on a thin, flexible substrate with a tuning circuit consisting of capacitive-coupled biasing tracks on the backside. Capacitive coupling isolates circuits at DC while providing connectivity at radio frequency (RF). Tracks act as the capacitors for the tuning biasing circuit. A double-sided copper clad Mylar substrate is etched to produce the slot antenna on one side and the biasing circuit using inexpensive Varactor diodes on the other side. The antenna tunes over a wide frequency range of approximately 2:1. The antenna is able to sense currents by providing a frequency response when connected to the sensing system. The current sensing antenna can also detect the operational or non-operational states of the appliances and devices. This low-cost setup of antenna on a flexible substrate can assist in detecting the power and current monitoring in household electrical devices providing an energy-efficient solution while also operating as a transmitter via Bluetooth. The measured reflection coefficients and radiation patterns are in a good agreement with the simulated results and noticeably clear sensing of current is achieved.



**Index Terms**— Tuning, Current Sensing, Sensing Antenna, Diodes, Smart Sensing System

## I. Introduction

ANTENNA designs that can accommodate several adjoining frequency bands are of great interest for current and future indoor and outdoor applications [1]. There are readily available means by which antennas accommodate multiple frequency bands such as multiband antennas and reconfigurable antennas. Multiband antennas operate at many bands simultaneously whereas reconfigurable antennas work by dynamically selecting the frequency operation [2]. Active alterations to the frequency of operation makes the reconfigurable antennas appropriate for multiple applications at the same time. A variety of methods have been implemented to realise the concept of frequency reconfigurability for instance: Micro-Electromechanical Systems (MEMS) [3], [4] liquid crystals [5], mechanical means [6], changing substrate characteristics [7], [8], using switching diodes [9] – [14] and varactor diodes [15] – [20]. Their versatile range and broad prospects of implementation, reconfigurable antennas can be particularly useful in radar, communication, shielding and security systems, smart surfaces and they can also be implemented in smart domestic appliance systems.

With the ever-expanding numbers of inhabitants across the planet, the demand for energy has witnessed a rapid rise. The gap between the excessive demands and inadequate supplies has caused plenty of excessive workload on the existing power plants resulting in significantly higher carbon emissions. Smart energy sensors and meters can be one of the potential solutions

in developing energy efficient appliances [21], and intelligent networks [22]. RFID based sensors for domestic electronic appliances have been frequently reported as a likely solution for smart sensing [23] – [27]. Some of the proposed solution possess the need for expensive external input of power supply to become operational [23] – [25] and thereby, increasing the system cost and reducing the energy efficiency. Some RFID solutions deploy high-priced microcontrollers and Analog-to-Digital (A2D) converters [26], [27] which bypass the necessity for external inputs of power supply but increase the expenses by the means of expensive components and microcontrollers. Analysis of the energy usage behaviour through the usage of smart plugs in combination with home energy management systems (HEMS) is presented in [28]. An example of a smart plug (Monjolo) where the energy for the sensor is harvested from the mains is described in [29]. Similarly, a battery-free, non-intrusive power meter for inexpensive energy monitoring with transmissions based on a LoRa system is proposed in [30]. Reconfigurable antennas have also been presented for sensing applications and tend to deploy extensive options ranging from no diodes [31] to two PIN diodes [32] to three diodes [33] however, all these sensing antennas tend to primarily offer the ON and OFF states of the sensing features of their respective designs.

This paper presents a reconfigurable slot antenna in a sensing system that can perform dual functions of sensing AC current levels as well as transmitting the data wirelessly over Bluetooth. This is a novel concept for potential sensing applications using

This work was funded by UK EPSRC High Value Manufacturing Fellowship (REF: EP/L017121/1), Royal Society-International Exchanges 2019 Cost Share (NSFC) (Ref: IEC\NSFC\191780) and CHIST ERA WISDOM project under EPSRC grant EP/P015840/1.

Anshuman Shastri, Irfan Ullah and Benito Sanz-Izquierdo are affiliated with the School of Engineering and Digital Arts, University of Kent, Canterbury CT2 7NT, United Kingdom (e-mail: [as2256@kent.ac.uk](mailto:as2256@kent.ac.uk); [iu22@kent.ac.uk](mailto:iu22@kent.ac.uk); [b.sanz@kent.ac.uk](mailto:b.sanz@kent.ac.uk)).

a standard reconfigurable antenna. The antenna is designed and fabricated on flexible substrate with the view of further integration within the cables and the rest of the sensing system. The antenna deploys capacitive coupling to simplify the biasing circuit and reduce the number of components on the flexible substrate. The reconfigurable antenna is able to tune over a wide range of frequencies which is ideal for current sensing applications. The AC current sensing antenna is used in the novel sensing setup comprising of a current transformer fitted with an AC/DC convertor to sense the AC current passing through the wire. The DC current is then converted to a DC voltage that is used to tune the frequency response of the reconfigurable antenna. This newly proposed sensing system provides a simple, cost-effective solution for a current sensing system for smart appliances for energy efficient homes.

## II. RECONFIGURABLE ANTENNA

### A. Antenna Design and Dimensions

Slot antennas are well-known structures that are widely used in communication systems. The knowledge of these antennas is constantly expanding and has recently been analysed in terms of characteristics modes [34]. The wideband tuning characteristic responses of reconfigurable slot antennas [1] make them highly beneficial for a prospective use as sensors. Here, a slot antenna design with a capacitive-coupled biasing on a thin flexible substrate is used to simplify the tuning circuit and to adapt to the sensing applications. The initial design can be seen from Fig. 1. A broad view of this antenna and the layout of the biasing tracks for tunable antennas is presented here in Fig. 1 where Fig 1 (a) shows the cross-section view, Fig. 1 (b) the backside and Fig. 1 (c) the face of the antenna with dimensions shown in Table I. The slot is etched on the top layer while the biasing tracks with the diode (in purple) and square patches (in black) are developed on the back layer to attach the coaxial port (in orange).

The antenna design was simulated using the time domain solver available in CST microwave studio™. The diode was computed as a lumped element using an equivalent circuit model for the BB857 Varactor diode [35] in reverse bias. Varactor diodes are also referred to as varicap diodes that demonstrate variable capacitance with the variation in the reverse bias voltage.

### B. Close-Coupled Biasing Technique

The capacitive-coupled biasing technique is attained by using two conductive tracks running along parallel to the slot. This biasing technique has previously been demonstrated in Frequency selective Surfaces in [36] and is implemented in switching antenna in [14] and is presented for tunable antennas for the first time here. Using extremely thin substrate in comparison to the wavelength allows the biasing tracks to be considered connected to the top metallic layer comprising of the slot at RF.

At DC, however, the biasing circuitry is completely isolated from the circuitry on the top layer. That prevents any connection amongst the two layers which simplifies the biasing circuit. This avoids any sort of connection between the two layers which abridges the biasing circuit significantly.

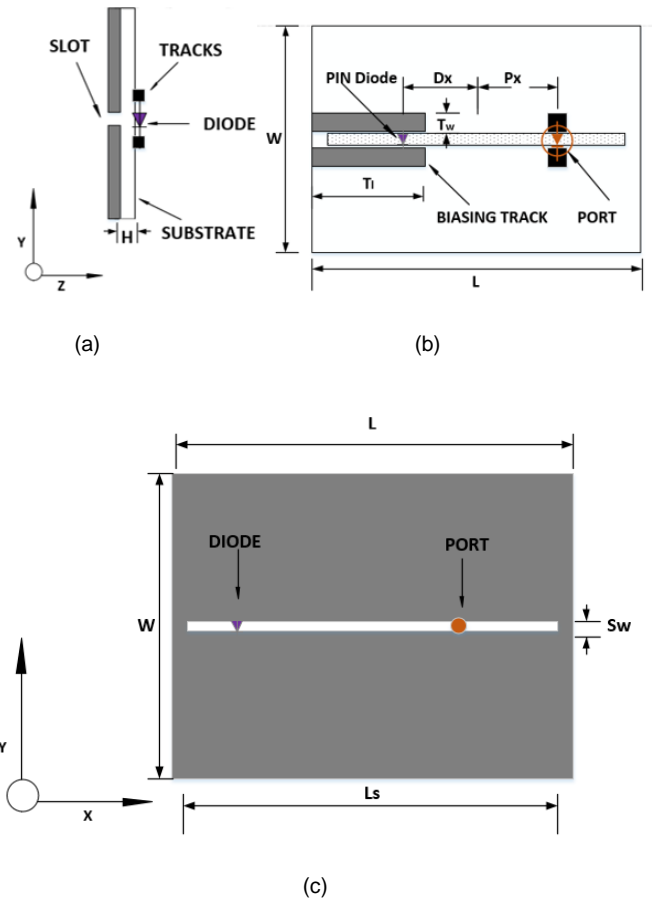


Fig. 1. Switchable antenna design with side view (a) back view (b) and front view (c)

TABLE I

ANTENNA DIMENSIONS

Length	L <sub>s</sub>	S <sub>w</sub>	L	W	P <sub>x</sub>	D <sub>x</sub>	T <sub>l</sub>	T <sub>w</sub>
Dimensions (mm)	65.4	0.5	69.4	47	15.8	30.7	15	3.5

The capacitance between each track and the ground plane containing the slot can be calculated using the Faraday's equation for the capacitance for two parallel plates:

$$C = (\epsilon_0 \epsilon_r A) / d \quad (1)$$

Where  $A$  stands for the area of the biasing track and  $d$  refers to the distance between the tracks and the ground.  $\epsilon_0$  and  $\epsilon_r$  denote the permittivity of the free space and the relative permittivity of the material, respectively. Value for  $\epsilon_0$  remains constant at  $8.854 \times 10^{-12} \text{ F} \cdot \text{m}^{-1}$  whereas the  $\epsilon_r$  value for the Mylar substrate is 3.1. The Mylar substrate has a thickness of 0.05 mm. The equation (1) gives a capacitance of approximately 10.3 pF for a track of dimensions of 15 mm by 3.5 mm and the subsequently impedance value for the tracks as approximately  $6.4 \Omega$  at 2.4 GHz. Using a Mylar substrate which had a thickness of 0.05 mm ( $0.0004 \lambda$ ) was a perfect solution for the choice of substrate to demonstrate close-coupled biasing technique for this application as the biasing between the layers was lost as the thickness was increased beyond  $0.001 \lambda$ . The

extremely thin slot antenna design can also be made foldable or flexible in nature which can be utilized to mount the antenna around a wire or within an appliance.

### C. Simulation Results and Analysis

The simulated  $S_{11}$  results can be seen in the Fig. 2. The resonant frequency of operation varies from 2.53 GHz for a capacitance value of 0.5 pF all the way to 1.4 GHz for a value of 6.6 pF. The value of the frequency gradually decreases with the increase in capacitance that can be tracked using the following fitting equation:

$$f = -0.1895C + 2.5497 \quad (2)$$

Where  $f$  stands for the frequency of operation whereas  $C$  represents the capacitance. In terms of bandwidth, higher capacitance value yields a lower -10 dB bandwidth up to 4pF mark after which the curve stabilizes.

The simulated surface currents at three resonant frequencies for 0.5 pF, 4 pF and 6.6 pF can be seen in Fig. 3. Surface currents clearly denote the surface current intensity at its highest in the area around the diode and around the location of the port. The current density gradually reduces as the capacitance value is increased. The density of the surface currents is at its highest at 0.5 pF and at its lowest when the capacitance is at 6.6 pF.

### D. Antenna Fabrication

The design was etched on a double-sided copper clad Mylar substrate of 0.05 mm thickness. This type of substrate is flexible and is ideal to shape and mount around surfaces if required. The coaxial cable along with the BB857 PIN diodes were added at the backside. The antenna design can be seen in Fig. 4. The etched antenna was mounted on a piece of Polystyrene foam for durability. 47 nH inductors are also mounted at the end of biasing tracks with the connecting wires for DC isolation, biasing circuit, and the wired connection necessary to for supply voltage. At the end of the inductors, two wires were extended for supply voltage and a 1 kΩ resistor was added to control the flow of current going into the diode.

### E. Reconfigurable Antenna Measurements

The reflection coefficient ( $S_{11}$ ) of the frequency reconfigurable antenna was measured using an R&S® ZVL135 Vector Network Analyzer by applying an external DC voltage supply which was varied manually to alter the effective capacitance of the Varactor.

When the voltage supply was varied from 28 V to 0 V, the antenna was able to detect the variation in voltage by presenting a change in the frequency of operation by altering the effective capacitance of the diode, thereby tuning the antenna at the frequency corresponding to the voltage and capacitance. The corresponding  $S_{11}$  is shown in Fig. 5. The resonant tuning frequencies in first mode range from 1.4 GHz to 2.5 GHz with a tuning ratio of 1.8:1 for the specified range of voltages. Resonant frequencies in the second mode ranged from 2.5 GHz to 4.3 GHz with the same tuning ratio of 1.8:1.

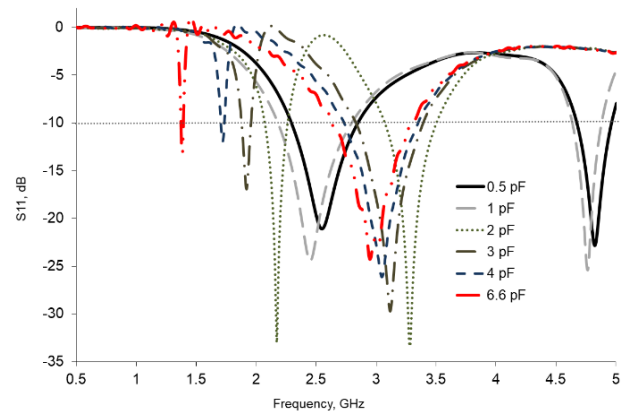


Fig. 2. Simulated reflection coefficient ( $S_{11}$ ) results for the capacitance range of 0.5 - 6.6 pF

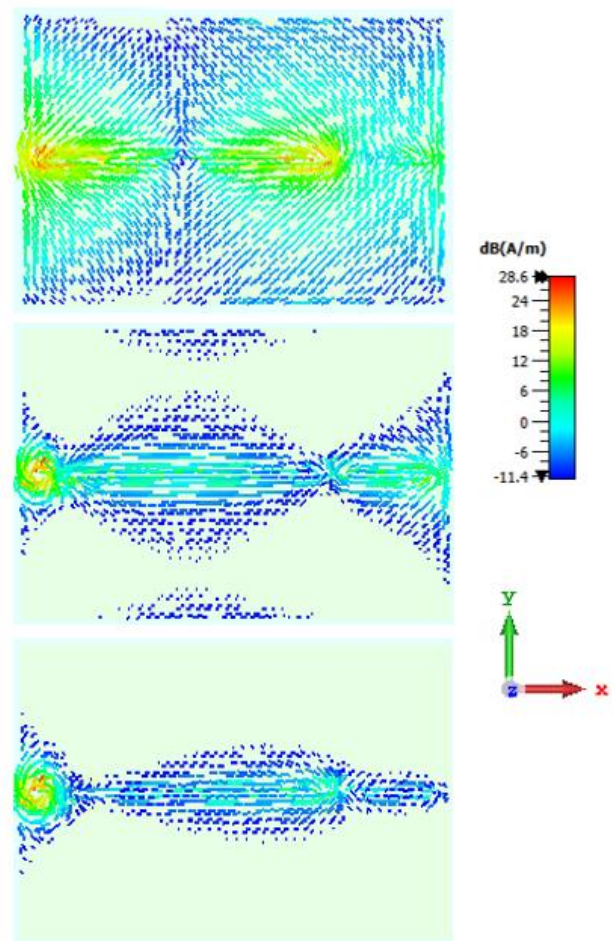
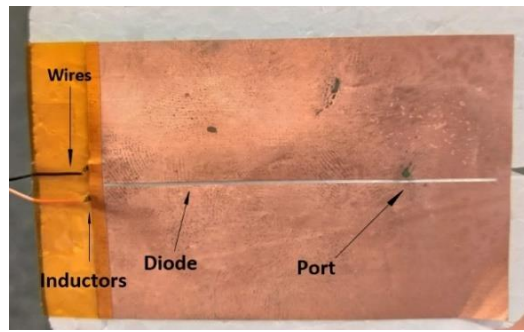
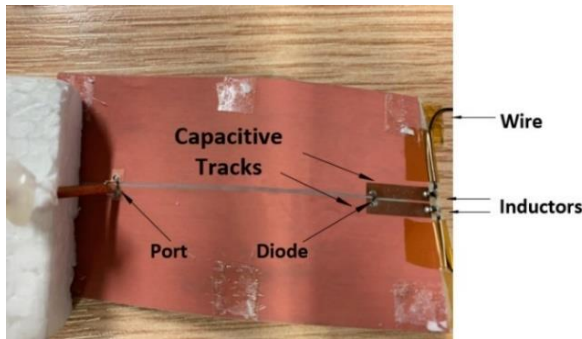


Fig. 3. Simulated Surface currents for the first mode at 0.5 pF (top), 4 pF (middle) and 6.6 pF (bottom) respectively

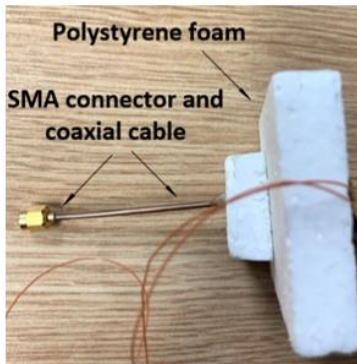
The measurement results correspond comparatively well to the expected results for capacitance presented in Fig. 2. An overall shift range of 1-6% was observed. The shift was minimal at 2 pF and 3 pF and more than 3% beyond 3 pF.



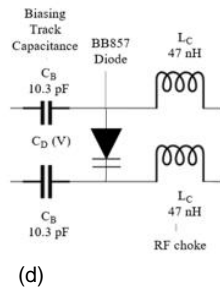
(a)



(b)



(c)



(d)

Fig. 4. Etched antenna design showing the SMA connector and extension wire (a) front, (b) side, (c) back and (d) equivalent biasing network schematics

Voltage versus capacitances relationship of the BB857 diodes is presented in Fig. 6. The small differences in the results are caused by the physical characteristics (encapsulate) of the diode at RF, which were not included in simulations.

A relationship between the simulated and measured voltage versus frequency and simulated and measured bandwidth is presented in Fig. 7. The values for the simulated voltage versus frequency were obtained using the capacitance in Fig. 2 and converting to voltage through the relationship in the graph in Fig. 5. Measured frequency of operation drastically increases with the increase in supply voltage up to 10 V as the increase in voltage leads to a decrease in capacitance. From 10 V onwards, the increase in the frequency slows.

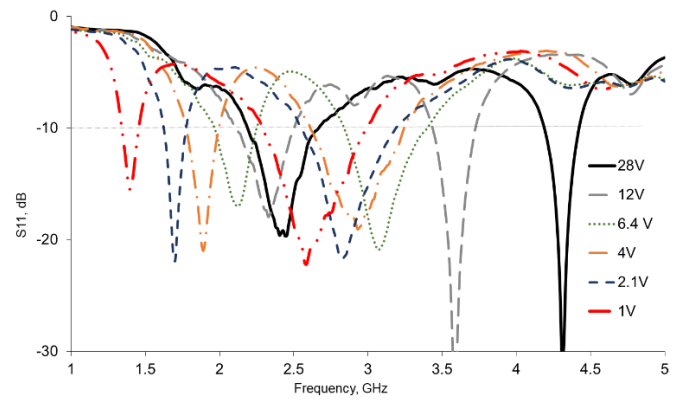


Fig. 5. Measured reflection coefficient at the corresponding Voltages

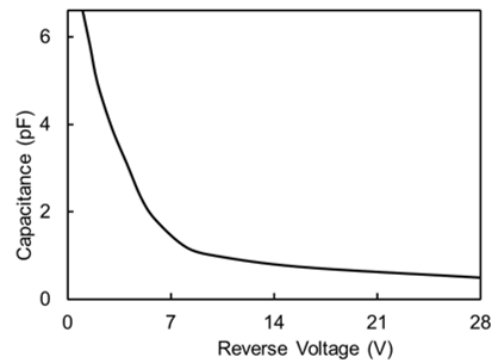


Fig. 6. Relationship between reverse biased voltage and capacitance of BB857 diode [35]

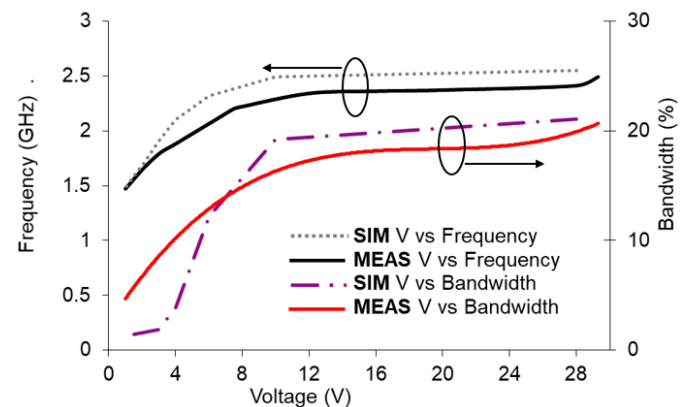


Fig. 7. Voltage vs Frequency vs Bandwidth relationship for simulated and measured results

The trend goes in coherence with the measured reflection coefficient ( $S_{11}$ ) results in which a small change between 28 V and 12 V was observed and a drastic shift was seen in the frequency of operation as the voltage varied between 12 V and 1 V. The capacitance-voltage correlation here is coherent with the results expected from their relationship as seen in Fig. 6 as well as Fig. 7. The corresponding voltages for the capacitance values were 12 V for 1 pF, 6.4 V for 2 pF, 4 V for 3 pF, 2.1 V for 4 pF and 1 V for 6.6 pF, respectively. The bandwidth shows a consistent curve which progressively increase with an increase in supply voltage.

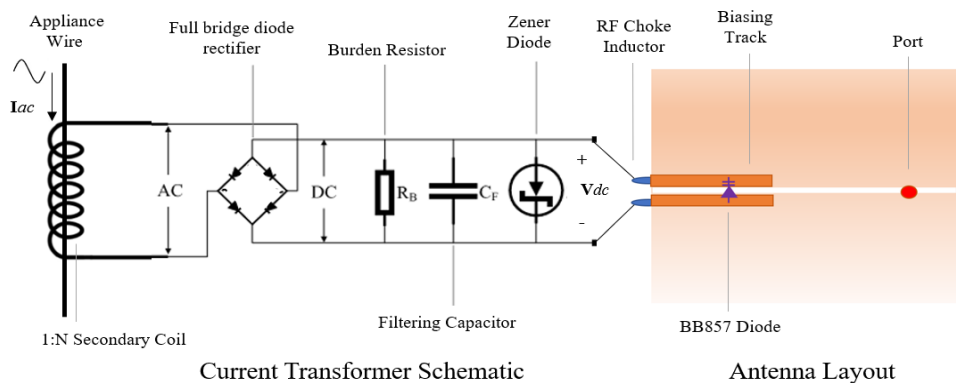


Fig. 8. Equivalent circuit schematics of the CT connected to the reconfigurable antenna

### III. AC CURRENT SENSING AND RADIATION CHARACTERISTICS

#### A. Current Sensing System

The current sensing setup incorporates the antenna with a current transformer (CT). An initial solution for UHF RFID sensors was proposed in [37]. The emphasis here is on implementing the setup using a reconfigurable antenna which can transmit at the Bluetooth band for smart phone communications. The schematic layout of the current sensing system is shown in Fig. 8 which encompasses three key elements: (I) Sensor transformer coil, (II) rectifier and filtering circuit, and (III) Reconfigurable antenna. Current transformer contains the elements I and II. It is employed to detect the AC current coming through a cable and convert it into DC voltage. This voltage is then used to control the reactance of the varactor diode in the tuning circuit of the antenna.

The physical implementation of Fig. 8 can be seen in Fig. 9. CT is connected to the reconfigurable antenna as well as an AC current wire. The biasing tracks of the antenna are not visible in the photo but were presented earlier in in Fig. 4 (b). The CT provides a linear correlation between the input current and DC output voltage under ideal conditions and by using those relations, a solution is proposed for AC current sensing applications that senses current over first band and transmits the recorded data over Bluetooth channel with the help of a voltage switch. The amphibious reconfigurable antenna operates as a part of the current sensing setup using the supply DC voltage converted from AC current from the appliance wire using CT or as a standalone sensing antenna using external DC voltage supply. A typical split-core CT with full bridge rectifiers senses the input current passing through an appliance wire and transforms the current value to a DC voltage output [38]. This readily available CT detects the input currents over the range of 0 A to 10 A and converts that into a 0 V to 10 V DC output. The CT packaging also consists of a burden resistor, a Zener diode, and a low-pass filter. The Zener diode controls the DC voltage output to a safe limit of 15 V to prevent the sudden spikes of voltages across the output. Two M3 screw terminals are mounted in CT over the removable cover that act that as the voltage output points.

BB857 Varactor diodes offer a wide range of variable capacitance across the voltage. Reverse biased voltage with diode capacitance is linear from 1 V to 7 V as seen in Fig. 6.

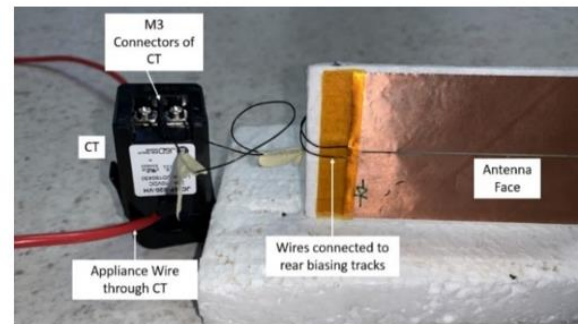


Fig. 9. Reconfigurable antenna connected with split wires and CT

#### B. Current Sensing Measurements

The current sensing measurement system employed is shown in Fig. 10. It consisted of a switchable standard electric heater load, a variac to change the supply AC current, an ABS box [39] containing the CT and the reconfigurable antenna. The CT was enclosed in the ABS box on health and safety grounds. The two output wires from the CT were extended outside the box from the M3 screws to connect to the antenna. The antenna was connected to a VNA to measure the reflection coefficient ( $S_{11}$ ).

Due to the type of switchable electric load available within the health and safety concerns, only measurements from 1-8 A were possible. A range of up to 10 A can be achieved if higher powered loads can be deployed. A commercial Brennenstuhl PM 231 E current meter [40] was employed at the power supply to monitor the AC current going through in the system. Expected and measured input current and output voltage characteristics of the system through CT can be seen in Fig. 11.

These results establish a relationship between the expected and actual V-I characteristics of the CT. The figure denotes that although the trend of the increasing output DC voltage maybe consistent with the expected trend in Fig. 11, a lower output DC voltage was delivered at the antenna. Lower voltage levels are observed due to the losses incurred across the switchable electric heater and due to the coupling with the antenna components such as wires, tracks and inductors. The AC current versus the resonant frequency of the antenna is illustrated in Fig. 12. Frequency and the AC current values demonstrate a linear relationship with a steady increase in the frequency of operation with an increase in AC current supply.

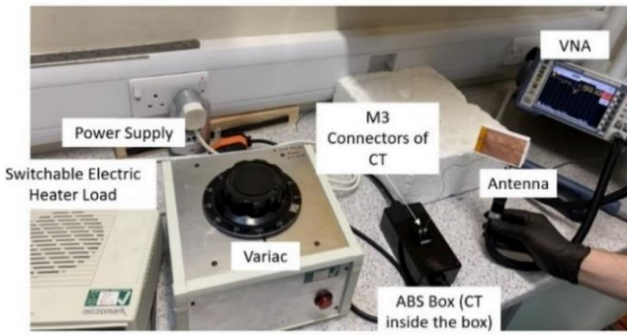


Fig. 10. AC Current sensing measurement system set up

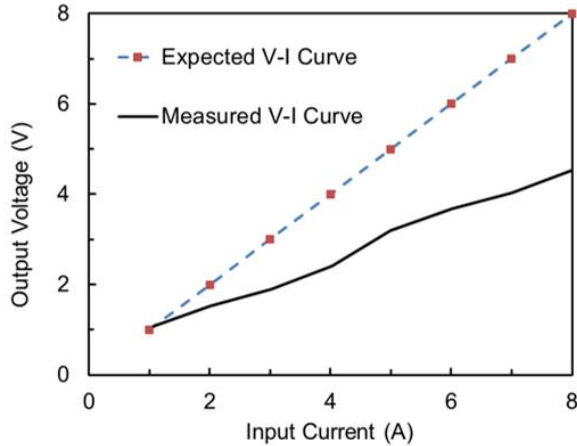


Fig. 11. Expected and measured AC current input and DC output voltage for CT

The corresponding measured reflection coefficient response using the current sensing system is presented in Fig. 13. The results correspond to the results obtained in Fig. 12. A noteworthy shift towards the lower band was observed beyond 1 A current due to the actual received voltage at the antenna being lower than expected as evident from Fig. 11. The relation between the shift in voltage was determined through the measured voltage at the specific current values. Whilst the frequency of the first mode varies as the supply current changes, the second mode is mostly stable and covered the below -10 dB bandwidth at or around 2.5 GHz frequency band for currents up to 6 A.

### C. Wireless Transmission at 2.5 GHz

Transmission at the bluetooth band within the 2.4 GHz to 2.5 GHz range can take place by switching from the sensing mode to transmission mode when supplied with an external supply of 28 V. This 28 V input can also be delivered with the help of a separate transformer connected to the mains AC voltage. By doing that, sensing voltage fluctuations for power measurements are also possible within the same system. Extremely little current of 10 nA is required for the varactor diode to operate and therefore, the external supply requires very low power which can be integrated within the system. Radiation patterns at 2.5 GHz can be seen in Fig. 14.

Radiation patterns at 2.5 GHz operational frequency were obtained by using an external DC voltage supply of 28 V. These radiation patterns are useful for the transmission option where the reconfigurable antenna can be connected to a DC battery supplying 28 V.

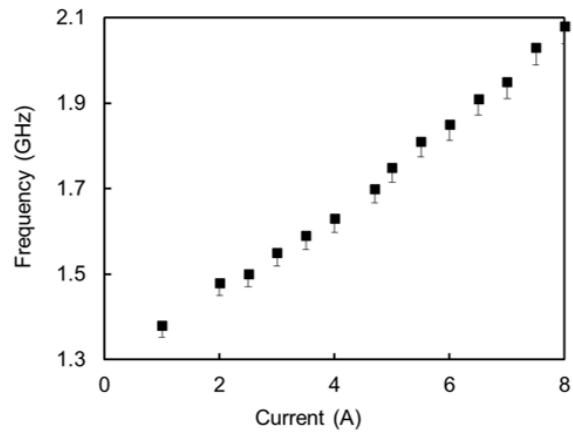


Fig. 12. Current Sensing Measurements

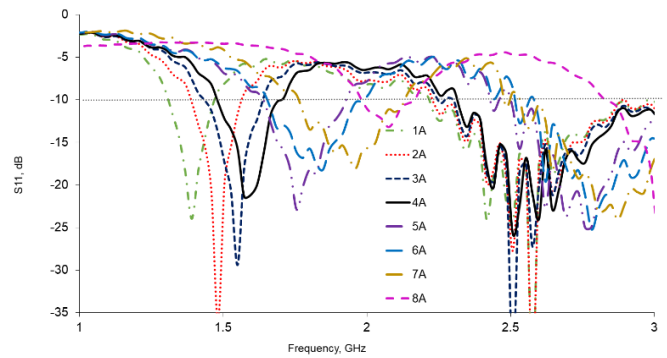


Fig. 13. Sensing Reflection coefficient measurements using the current sensing setup measuring 1-8 A

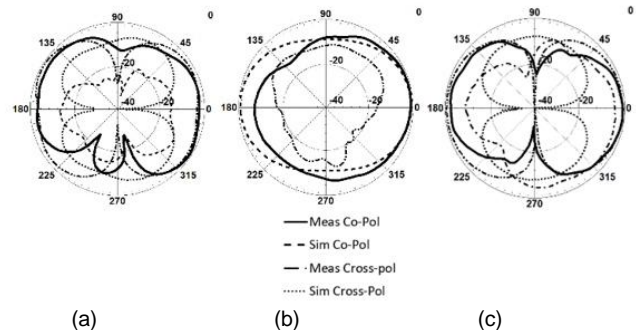


Fig. 14. First band measured and simulated radiation patterns at 28 V for 2.5 GHz for the antenna in (a) XY-plane, (b) XZ-plane and (c) YZ-plane

Radiation Patterns are in coherence with the expected results of a complementary dipole which is fed by a coaxial cable from the rear. The patterns are mainly omnidirectional in the XZ-plane with unequal lobes due to the presence of the coaxial cable and SMA connector at the rear of the antenna.

Finally, a table comparing existing smart sensors with proposed AC sensing antenna system is presented as Table II. A range of smart sensors are compared in terms of their types, frequencies of operation, direct tuning capabilities, antenna sensing, and their requirements for powering, referred as power style. The proposed antenna combined transmission and sensing within the same antenna and provided broadband sensing that offers superior sensitivity. Proposed antenna was the only one that provided a direct tuning across its entire wide frequency range while providing foldability and flexibility.

TABLE II

COMPARISON OF SMART POWER SENSING SYSTEMS AND PROPOSED SENSING ANTENNA SYSTEM

Ref.	Sensor Type	Frequencies of Operation	Direct Antenna Tuning Range	Sensing Antenna	Power Style
[29]	Energy-Harvesting Metering Sensor	868 MHz	No	No	Passive
[25]	Wireless, powerless RFID	850 MHz – 950 MHz	No	No	Passive
[30]	Clamp-on Inductive current sensor	Not available (LoRa Based)	No	No	Passive
[27]	ZigBee based controller	2.4 GHz	No	No	Active
[37]	Sensor code-based RFID	768 MHz – 868 MHz	1:1 Sensor code	Yes	Passive
<b>This Slot Ant.</b>	<b>Proposed AC sensing antenna system</b>	<b>1.38 GHz – 2 GHz sensing. 2.45 GHz transmit</b>	<b>2:1</b>	<b>Yes</b>	<b>Active (Passive possible)</b>

#### IV. CONCLUSION

A dual-operation concept for current sensing and transmission using a reconfigurable slot antenna has been demonstrated. The novel sensing setup can sense AC currents in an electric cable of a smart domestic appliance or other electrical device. The reconfigurable antenna is able to provide a wide frequency response as a function of voltage with a tuning ratio of 2:1. This wide frequency of operation can be split so that the lower frequencies can be utilised for sensing while the higher frequencies can be used for transmission at the 2.4 GHz Bluetooth band. The Bluetooth band was selected because it is used in smartphone technologies and for domestic applications, the level of interference stays relatively low. ZigBee is another technology that could be incorporated as it operates in the same band and it may perform well in terms of interference, particularly for smart home networks.

In order to sense current, an AC current transformer (CT) has been connected directly to the active circuit of the reconfigurable antenna. A linear and consistent relationship between the current sensing and frequency of operation has been obtained for the range of frequency allowed within the system setup. At the transmitting band at 2.4 GHz, the radiation patterns are the expected ones for a slot antenna and is mostly omnidirectional in the XZ-plane. The slight variations in simulation and measurement results were present owing to the use of the inexpensive components and unavoidable design features such as the effect of moving extension wires. The complete encapsulation aspects of the diodes and the moving extension wires considerations were not included in the simulation studies.

In terms of the reconfigurable antenna, a further innovation by using a capacitive-coupling biasing technique to simplify the tuning is demonstrated. Low-cost flexible substrates and active components such as the ones employed are desirable for this application. The flexible nature of the antenna can allow the antenna to be compactly rolled around the wire or mounted over the appliance surface for better utilisation of space. The wideband sensing of the antenna provides a one-stop-shop solution for the smart domestic appliance network that can save energy significantly. The potential ability of the antenna to detect current in the first band and transmit results using the Bluetooth second band presents another exciting solution for smart domestic appliances.

#### ACKNOWLEDGMENT

The authors would like to thank Mr. Simon Jakes and Mr. Antonio Mendoza for their assistance during fabrication and measurements.

#### REFERENCES

- [1] J. Bernhard, Reconfigurable antennas, 1st ed. San Rafael, Calif: Morgan & Claypool Publishers, 2007, pp.1-74.
- [2] M. A. Matin, Wideband, multiband, and smart reconfigurable antennas for modern wireless communications. Hershey, PA: Information Science Reference, 2016.
- [3] B. A. Cetiner, G. R. Crusats, L. Jofre, and N. Biyikli, "RF MEMS integrated frequency reconfigurable annular slot antenna," *IEEE Trans. Antennas Propag.*, vol. 58, no. 3, pp. 626–632, Mar. 2010.
- [4] E. Erdil, K. Topalli, M. Unlu, O. A. Civi, and T. Akin, "Frequency tunable patch antenna using RF MEMS technology," *IEEE Trans. Ant. Propag.*, vol. 55, no. 4, pp. 1193–1196, Apr. 2007.
- [5] R. Bose, and A. Sinha, "Tunable patch antenna using a liquid crystal substrate", Radar Conference, 2008, RADAR '08, IEEE, 26-30 May 2008, pp.1-6.
- [6] A. Semnani, M. D. Sinanis and D. Peroulis, "An Evanescent-Mode Cavity-Backed High-Power Tunable Slot Antenna," in *IEEE Transactions on Antennas and Propagation*, vol. 67, no. 6, pp. 3712-3719, June 2019, doi: 10.1109/TAP.2019.2905738.
- [7] G. H. Huff, D. L. Rolando, P. Walters, and J. McDonald, "A frequency reconfigurable dielectric resonator antenna using colloidal dispersions", *IEEE Antennas and Wireless Propagation Letters*, Vol. 9, 2010, pp. 288-290.
- [8] D. M. Pozar, and V. Sanchez, "Magnetic tuning of a microstrip antenna on a ferrite substrate", *Electronics Letters*, Vol. 24, Issue 12, 9th June 1988, pp.
- [9] H. A. Majid, M. K. A. Rahim, M. R. Hamid, N. A. Murad, M. F. Ismail, "Frequency reconfigurable microstrip patch-slot antenna", *IEEE Antennas Wireless Propag. Lett.*, vol. 12, pp. 218-220, 2013.
- [10] L. Pazin and Y. Leviatan, "Reconfigurable Slot Antenna for Switchable Multiband Operation in a Wide Frequency Range", *EEE Antennas Wireless Propag. Lett.*, vol. 12, pp. 329-332, 2013.
- [11] D. Peroulis, K. Sarabandi, and L. P. B. Katehi, "Design of reconfigurable slot antennas", *IEEE Trans. Antennas and Propag.*, vol. 53, Feb. 2005, pp. 645-654.
- [12] M. Shirazi, J. Huang, T. Li, and X. Gong, "A Switchable-Frequency Slot-Ring Antenna Element for Designing a Reconfigurable Array," *EEE Antennas Wireless Propag. Lett.*, vol. 17, no. 2, pp. 229–233, 2018.
- [13] N. Symeon, R. Bairavasubramanian, C. Jr. Lugo, I. Carrasquillo, D. C. Thompson, G. E. Ponchak, J. Papapolymerou, and M. M. Tentzeris, "Pattern and frequency reconfigurable annular slot antenna using PIN diodes", *IEEE Trans. Antennas and Propag.*, vol. 54, Feb. 2006, pp. 439-448.
- [14] A. Shastri, B. Sanz-Izquierdo, D. Atkins and A. McClelland, "Frequency Reconfigurable Double-sided Slot Antenna Using Close-coupled Biasing Technique," *2018 8th IEEE India International Conference on Power Electronics (IICPE)*, Jaipur, India, 2018, pp. 1-4, doi: 10.1109/IICPE.2018.8709598.

- [15] M. F. Farooqui and A. Kishk, "3-D-Printed Tunable Circularly Polarized Microstrip Patch Antenna," in *IEEE Antennas and Wireless Propagation Letters*, vol. 18, no. 7, pp. 1429-1432, July 2019, doi: 10.1109/LAWP.2019.2919255.
- [16] S. Kawasaki and T. Itoh, "A slot antenna with electronically tunable length", 1991 Antennas and Propagation Society Symp., 24-28 June 1991.
- [17] N. Behdad and K. Sarabandi, "A Varactor-Tuned Dual-Band Slot Antenna", *IEEE Trans. Antennas and Propag.*, vol. 54, no. 2, pp. 401-408, 2006.
- [18] J. Yang, W.-W. Choi, and K.-W. Tam, "A novel dual-band frequency tunable slot antenna with constant frequency ratio," 2015 Asia-Pacific Microwave Conference (APMC), 2015.
- [19] C. R. White and G. M. Rebeiz, "Single- and Dual-Polarized Tunable Slot-Ring Antennas", *IEEE Trans. Antennas and Propag.*, vol. 57, no. 1, pp. 19-26, 2009.
- [20] A. H. Mohammadi and K. Fororaghi, "A varactor-tuned substrate-integrated cavity-backed dumbbell slot antenna," *2012 15 International Symposium on Antenna Technology and Applied Electromagnetics*, 2012.
- [21] M. Zeifman and K. Roth, "Nonintrusive appliance load monitoring: Review and outlook," in *IEEE Transactions on Consumer Electronics*, vol. 57, no. 1, pp. 76-84, February 2011, doi: 10.1109/TCE.2011.5735484.
- [22] J. Leitão, P. Gil, B. Ribeiro and A. Cardoso, "A Survey on Home Energy Management," in *IEEE Access*, vol. 8, pp. 5699-5722, 2020, doi: 10.1109/ACCESS.2019.2963502.
- [23] M. Kuzlu, M. Pipattanasomporn and S. Rahman, "Hardware demonstration of a home energy management system for demand response applications", *IEEE Trans. Smart Grid*, vol. 3, no. 4, pp. 1704-1711, Dec. 2012.
- [24] R. Vyas *et al.*, "Inkjet Printed, Self Powered, Wireless Sensors for Environmental, Gas, and Authentication-Based Sensing," in *IEEE Sensors Journal*, vol. 11, no. 12, pp. 3139-3152, Dec. 2011, doi: 10.1109/JSEN.2011.2166996.
- [25] B. S. Cook *et al.*, "RFID-Based Sensors for Zero-Power Autonomous Wireless Sensor Networks," in *IEEE Sensors Journal*, vol. 14, no. 8, pp. 2419-2431, Aug. 2014, doi: 10.1109/JSEN.2013.2297436.
- [26] J. Cheng, M. Hung and J. Chang, "A ZigBee-Based Power Monitoring System with Direct Load Control Capabilities," *2007 IEEE International Conference on Networking, Sensing and Control*, London, 2007, pp. 895-900, doi: 10.1109/ICNSC.2007.372900.
- [27] J. Han, H. Lee and K.-R. Park, "Remote-controllable and energy-saving room architecture based on ZigBee communication," *2009 Digest of Technical Papers International Conference on Consumer Electronics*, Las Vegas, NV, 2009, pp. 1-2, doi: 10.1109/ICCE.2009.5012332.
- [28] S. Zhai, Z. Wang, X. Yan and G. He, "Appliance Flexibility Analysis Considering User Behavior in Home Energy Management System Using Smart Plugs," in *IEEE Transactions on Industrial Electronics*, vol. 66, no. 2, pp. 1391-1401, Feb. 2019, doi: 10.1109/TIE.2018.2815949.
- [29] S. DeBruin, B. Campbell, and P. Dutta, "Monjolo: An energy-harvesting energy meter architecture," in *Proc. SenSys*, Roma, Italy, Nov. 2013, pp. 18:1-18:14.
- [30] G. Dalpiaz, A. Longo, M. Nardello, R. Passerone and D. Brunello, "A battery-free non-intrusive power meter for low-cost energy monitoring," *2018 IEEE Industrial Cyber-Physical Systems (ICPS)*, St. Petersburg, 2018, pp. 653-658, doi: 10.1109/ICPHYS.2018.8390784.
- [31] X. L. Bao and M. J. Ammann, "Monofilar Spiral Slot Antenna for Dual-Frequency Dual-Sense Circular Polarization," in *IEEE Transactions on Antennas and Propagation*, vol. 59, no. 8, pp. 3061-3065, Aug. 2011, doi: 10.1109/TAP.2011.2158964.
- [32] A. Vamseekrishna, B. T. P. Madhav, T. Anilkumar and L. S. S. Reddy, "An IoT Controlled Octahedron Frequency Reconfigurable Multiband Antenna for Microwave Sensing Applications," in *IEEE Sensors Letters*, vol. 3, no. 10, pp. 1-4, Oct. 2019, Art no. 3502204, doi: 10.1109/LSSENS.2019.2943772.
- [33] B. P. Chacko, G. Augustin and T. A. Denidni, "Electronically Reconfigurable Uniplanar Antenna With Polarization Diversity for Cognitive Radio Applications," in *IEEE Antennas and Wireless Propagation Letters*, vol. 14, pp. 213-216, 2015, doi: 10.1109/LAWP.2014.2360353.
- [34] N. M. Mohamed-Hicho, E. Antonino-Daviu, M. Cabedo-Fabres, *et al.*, "Designing Slot Antennas in Finite Platforms Using Characteristic Modes," *IEEE Access*, vol. 6, pp. 41346-41355, 2018.
- [35] "Infineon BB857 Datasheet." [Online]. Available: [https://www.infineon.com/dgdl/Infineon-BB837\\_BB857SERIES-DS-v01\\_01-en.pdf?fileId=db3a304313d846880113d97339a9011a](https://www.infineon.com/dgdl/Infineon-BB837_BB857SERIES-DS-v01_01-en.pdf?fileId=db3a304313d846880113d97339a9011a). [Accessed: 27-Jul-2020].
- [36] B. Sanz-Izquierdo, E. Parker, J. Robertson and J. Batchelor, "Tuning technique for active FSS arrays", *Electronics Letters*, vol. 45, no. 22, p. 1107, 2009. Available: 10.1049/el.2009.2264.
- [37] I. Ullah, R. Horne, B. Sanz-Izquierdo and J. C. Batchelor, "RFID AC Current Sensing Technique," in *IEEE Sensors Journal*, vol. 20, no. 4, pp. 2197-2204, 15 Feb. 15, 2020, doi: 10.1109/JSEN.2019.2949856.
- [38] Magnelab. (Jul 27, 2020). *DCT-0016-10/10Vdc Split-Core Current Sensor*. [Online]. Available: <http://www.magnelab.com/products/acsplitcore-current-sensor-dct-0016-100/>
- [39] Dd Magnelab. (Jul. 27, 2020). *SCT-125w-100 by Magnelab*. [Online]. Available: <https://www.magnelab.com/products/wireless-ac-currentsensor-system-sct-125w/>
- [40] Brennenstuhl Smart Technology. (Jul. 19, 2020). *Primera-Line Wattage and Current Meter PM 231 E*. [Online]. Available: <https://www.brennenstuhl.co.uk/en-GB/products/adapter-plugs/primera-linewattage-and-current-meter-pm-231-e-gb>



**Anshuman Shastri** received the B.E.(Hons.) degree in Electronics and Communications Engineering from Birla Institute of Technology and Science, India in 2014 and the MSc by research degree in Electronics Engineering from University of Kent, U.K. in 2016.

He is a PhD Researcher at University of Kent, U.K. His research interests include microwave antennas, reconfigurable antennas, energy harvesting, additive manufacturing, frequency selective surfaces, millimetre wave devices and modelling of frequency reconfigurable structures.

He has worked as a visiting researcher and investigator as a member of a project headed by Dr. Benito Sanz-Izquierdo at Centre for Process Innovation, U.K. in 2018 where he developed microwave and millimetre wave frequency selective structures. He received the International Young Scientist Award for Electronics Engineering in 2020 for his contributions in electronics engineering and additive manufacturing.



**Irfan Ullah** received the B.Eng. (Hons.) degree in electronic and communications engineering from the University of Kent, Canterbury, U.K., in 2016, where he is currently pursuing the Ph.D. degree in electronic engineering.

His current research interests include small antennas, passive UHF RFID tag, and passive sensing devices.



**Benito Sanz-Izquierdo** received the B.Sc. from ULPGC (Spain), and the M.Sc. and Ph.D. degrees from the University of Kent, U.K., in 2002 and 2007, respectively.

From 2003 to 2012, he was Research Associate with the School of Engineering, University of Kent, he became a lecturer in Electronic Systems in 2013 and Senior Lecturer in 2019. In 2012, he worked for Harada Industries Ltd where he developed novel antennas for the automotive industry. His research interests are multiband antennas, wearable microwave devices, additive manufacturing, RF sensing, electromagnetic band-gap structures, and frequency selective surfaces.